Hindawi
Journal of Chemistry
Volume 2021, Article ID 2408006, 13 pages
https://doi.org/10.1155/2021/2408006

Research Article

Synthesis and Evaluation of the Antibacterial and Antioxidant Activities of Some Novel Chloroquinoline Analogs

Bayan Abdi,[1] Mona Fekadu,[1] Digafie Zeleke,[1] Rajalakshmanan Eswaramoorthy,[2] and Yadessa Melaku[1]

[1]*Department of Applied Chemistry, Adama Science and Technology University, P.O. Box 1888, Adama, Ethiopia*
[2]*Saveetha Dental College and Hospitals, Saveetha Institute of Medical and Technical Sciences, Poonamallee High Road, Chennai 600 077, Tamil Nadu, India*

Correspondence should be addressed to Yadessa Melaku; yadessamelaku2010@gmail.com

Received 11 November 2021; Revised 17 December 2021; Accepted 18 December 2021; Published 30 December 2021

Academic Editor: Liviu Mitu

Quinoline heterocycle is a useful scaffold to develop bioactive molecules used as anticancer, antimalaria, and antimicrobials. Inspired by their numerous biological activities, an attempt was made to synthesize a series of novel 7-chloroquinoline derivatives, including 2,7-dichloroquinoline-3-carbonitrile (**5**), 2,7-dichloroquinoline-3-carboxamide (**6**), 7-chloro-2-methoxyquinoline-3-carbaldehyde (**7**), 7-chloro-2-ethoxyquinoline-3-carbaldehyde (**8**), and 2-chloroquinoline-3-carbonitrile (**12**) by the application of Vilsmeier–Haack reaction and aromatic nucleophilic substitution of 2,7-dichloroquinoline-3-carbaldehyde. The carbaldehyde functional group was transformed into nitriles using $POCl_3$ and NaN_3, which was subsequently converted to amide using CH_3CO_2H and H_2SO_4. The compounds synthesized were screened for their antibacterial activity against *Staphylococcus aureus*, *Escherichia coli*, *Pseudomonas aeruginosa*, and *Streptococcus pyogenes*. Compounds **6** and **8** showed good activity against *E. coli* with an inhibition zone of 11.00 ± 0.04 and 12.00 ± 0.00 mm, respectively. Compound **5** had good activity against *S. aureus* and *P. aeruginosa* with an inhibition zone of 11.00 ± 0.03 mm relative to standard amoxicillin (18 ± 0.00 mm). Compound **7** displayed good activity against *S. pyogenes* with an inhibition zone of 11.00 ± 0.02 mm. The radical scavenging activity of these compounds was evaluated using 1,1-diphenyl-2-picrylhydrazyl (DPPH), and compounds **5** and **6** displayed the strongest antioxidant activity with IC_{50} of 2.17 and 0.31 μg/mL relative to ascorbic acid (2.41 μg/mL), respectively. The molecular docking study of the synthesized compounds was conducted to investigate their binding pattern with topoisomerase IIβ and *E. coli* DNA gyrase B. Compounds **6** (−6.4 kcal/mol) and **8** (−6.6 kcal/mol) exhibited better binding affinity in their *in silico* molecular docking against *E. coli* DNA gyrase. The synthesized compounds were also found to have minimum binding energy ranging from −6.9 to −7.3 kcal/mol against topoisomerase IIβ. The SwissADME predicted results showed that the synthesized compounds **5–8** and **12** satisfy Lipinski's rule of five with zero violations. The ProTox-II predicted organ toxicity results revealed that all the synthesized compounds were inactive in hepatotoxicity, immunotoxicity, mutagenicity, and cytotoxicity. The findings of the in vitro antibacterial and molecular docking analysis suggested that compound **8** might be considered a hit compound for further analysis as antibacterial and anticancer drug. The radical scavenging activity displayed by compounds **5** and **6** suggests these compounds as a radical scavenger.

1. Introduction

Pathogenic microorganisms, including bacteria, viruses, fungi, and protozoan, are the major cause of public health problems in developed and developing countries [1, 2]. Cancer and bacterial diseases are the leading cause of death all over the world. So far, numerous types of drugs have been developed and used to treat of various types of infections [3]. However, various reports have disclosed that pathogenic microorganisms develop resistance against most of commercially available drugs. The problem is exacerbated due to the emergence of new pathogenic microorganisms at an alarming rate [4]. In addition to pathogenic microorganism, free radicals also attack body's cells causing deleterious

diseases including cancer, cataract, premature aging, and other degenerative diseases [5, 6]. Thus, the treatment of infectious diseases and cancer remains challenging in this era and demand a continuous research to develop new, effective, and safe antibiotics [4].

Quinoline is an aromatic heterocyclic compound characterized by having a double-ring structure composed of benzene and a pyridine ring. For the last ten decades, quinoline moiety has been used as a scaffold for drug design and development. Even today, compounds containing this scaffold represent an inexhaustible inspiration for the design and development of novel semisynthetic or synthetic agents exhibiting a broad spectrum of bioactivities. Both natural and synthetic analogs of quinolines were reported to have several biological activities, including anticancer [7], antimalarial [8], antibacterial [7], antiviral [9], antifungal [10], and anti-inflammatory [10]. In drug development, choosing a correct molecular scaffold is one of the most important roles of chemists. Among several scaffolds, quinoline, with its good chemical reactivity and enormous biological activities, has been used as a starting point for drug synthesis or modification [11, 12]. Various types of functional groups can be introduced using relatively simple reactions [13]. Because of these attractive properties, to date, there are antibacterial [14], anticancer [15], and antimalarial [16] commercial quinoline-based drugs.

The broad spectrum biological activities of quinoline-based compounds urge the generation of a large number of structurally diverse derivatives. In this regard, quinoline-3-carbonitrile derivatives were reported as a valuable starting material for the development of broad-spectrum antibacterial agents [17]. The good antibacterial activities of derivatives of quinoline-3-carbonitrile were also reported by Khan et al. [17]. These reports further necessitate the synthesis of several analogs derived from the substitution of the 2-chloro in 2-chloroquinoline-3-carbaldehydes using various nucleophiles. In fact, the synthesis and biological activities of 2-chloro and 2,7-dichloroquinoline-3-carbaldehydes were also reported in the literature [18]. Inspired by the good biological activities of 2-chloroquinoline-3-carbaldehydes, we have previously reported the synthesis and antibacterial activities of various derivatives of quinoline-3-carbaldehydes [17]. Indeed, compounds with better antibacterial and antioxidant activities were synthesized [17]. The side chains of the benzene ring of quinolines are the other key focus area to build novel compounds with better biological activities. Owing to such significance and keeping in view the wide range of biological activities of chloroquinoline, we are interested in the synthesis of derivatives of quinolines having chlorine in the benzene ring. Herein, we reported the synthesis and biological activities of some novel 7-chloroquinoline derivatives. The *in silico* molecular docking analysis against *E. coli* DNA gyrase B and human topoisomerase IIβ and pharmacokinetic properties of the synthesized compounds were also incorporated for the first time in this paper.

2. Material and Methods

2.1. General. The chemicals used in this study were bought from Loba Chemie Pvt., Ltd. The Thiele tube was used to determine the melting point. The synthesized compounds were purified by column chromatography using silica gel (60–120 mesh) Merck. The progress of the reaction was monitored by TLC, and spots were detected using UV lamp. NMR analyses were carried out on Bruker Avance 400 MHz spectrometer using $CDCl_3$, MeOD-*d4*, and DMSO-*d6* as a solvent. Coupling constants *J* in Hz were directly calculated from the spectra. Splitting patterns are designated as *s* (singlet), *d* (doublet), *t* (triplet), *q* (quartet), and *m* (multiplet). Low-resolution electron impact mass spectra were obtained at 70 eV using a double focusing sector field mass spectrometer Finnigan MAT 95.

2.2. Synthesis

2.2.1. Synthesis of Acetanilide. In a 250 mL round flask, aniline (25 mL), acetic anhydride (25 mL), zinc powder (0.2 g), and acetic acid (25 mL) were added. The mixture was boiled under reflux using a water condenser for 2 hours. Then, it was cooled to room temperature and poured into 300 mL of crushed ice water. The solid product was collected by suction filtration (white crystals; yield 89%, mp 112–113°C (Lit. mp 114.3°C)) [19].

2.2.2. Synthesis of 3-Chloroacetanilide. In a 250 mL round flask, 3-chloroaniline (25 mL), acetic anhydride (25 mL), zinc powder (0.2 g), and acetic acid (25 mL) were added. The mixture was boiled under reflux using a water condenser for 2 hours. Then, it was cooled to room temperature and poured into 300 mL of crushed ice water. The solid product was collected by suction filtration (white crystals; yield 91%, mp 72–74°C (Lit. mp 76°C)) [20].

2.2.3. Synthesis of 2-Chloroquinoline-3-carbaldehyde. N,N-Dimethylformamide (21.1 mL, 0.27 mol) was added to a 250 mL round-bottom flask guarded with a drying tube; it was cooled to 0°C using an ice bath. Then, phosphorus oxychloride (60 mL, 0.64 mol) was added dropwise from the separatory funnel guarded by a drying tube while stirred by a magnetic stirrer. This addition was done for 30 minutes. Then, acetamide (12.34 g, 0.09 mol) was added. After 5 minutes, the dropper funnel was replaced by an air condenser with guarding tube at its end, and the mixture was heated for 22 hours on an oil bath at 94–98°C. Then, it was cooled to room temperature, poured into a beaker containing 400 mL crushed ice water, and stirred for 20 minutes. The yellow solid product was collected by suction filtration and washed with cold water. The crude yield was 14.6 g (83%) and recrystallized from ethyl acetate (yellow crystals; yield 5.2 g (30%), mp 146–148°C (Lit. mp 146–148°C)) [19].

*2.2.4. Synthesis of 2,7-Dichloroquinoline-3-carbaldehyde (**4**).* N,N-Dimethylformamide (16.5 mL, 0.21 mol) was added to a 250 mL round bottom flask guarded with a drying tube; it was cooled to 0°C using an ice bath. Then, phosphorus oxychloride (46.5 mL, 0.50 mol) was added dropwise from the separatory funnel guarded by a drying tube while stirred by a magnetic stirrer. This addition was done for 30 minutes. Then, N-(3-chlorophenyl)-acetamide (12 g, 0.07 mol) was added to it. After 5 minutes, the dropper funnel was replaced by an air condenser with guarding tube at its end, and the mixture was heated for 22 hours on an oil bath at 100–105°C. Then, it was cooled to room temperature, poured into a beaker containing 300 mL crushed ice water, and stirred for 20 minutes. The yellow solid product was collected by suction filtration and washed with cold water. The crude yield was 4.5 g (28%) and recrystallized from ethyl acetate; yellow crystals; mp 170–174°C; yield 2.38 g (15%); UV-Vis: λmax (MeOH) 324 nm; MS (EI, 70 eV) m/z 226; ^{1}H NMR (400 MHz, MeOD-d_4 and $CDCl_3$): δ_H 7.40 (1H, m, H-6), 7.75 (1H, m, H-5), 8.33 (1H, s, H-8), 8.58 (1H, d, J = 8.00 Hz, H-4) and 10.33 (1H, s, aldehyde proton); ^{13}C NMR (100 MHz, MeOD-d_4 and $CDCl_3$): δ_C 125.3 (C3), 126.3 (C-10), 129.2 (C-8), 130.8 (C-6), 136.0 (C-5), 140.2 (C-7), 141.7 (C-4), 147.0 (C-9), 151.4 (C-2), and 188.7 (carbonyl carbon).

*2.2.5. Synthesis of 2,7-Dichloroquinoline-3-carbonitrile (**5**).* 2,7-Dichloroquinoline-3-carbaldehyde (0.3 g, 1.3 mmol), sodium azide (0.13 g, 2 mmol), and phosphorus oxychloride (2 mL) were added to the test tube in 1 : 1:5 ratios. The mixture was stirred for 20 minutes and heated for 6 hrs in a water bath by checking the progress of reaction with TLC. The mixture was cooled and poured into the beaker containing 20 mL of crushed ice water with stirring. The product was filtered by suction filtration and washed with cold water. The yellow crystal product was collected by suction filtration (mp 150–156°C; yield 0.19 g (64%); TLC : R_f = 0.71 (n-hexane : ethyl acetate, 4 : 2)). The product was purified over silica gel column chromatography n-hexane : ethyl acetate (2 : 1) as eluent. UV-Vis λmax (MeOH) 359 nm; MS (EI, 70 eV) m/z 223; ^{1}H NMR (400 MHz, MeOD-d_4 and $CDCl_3$): δ_H 7.64 (1H, d, J = 8.00 Hz, H-6), 7.86 (1H, d, J = 8.00 Hz, H-5), 8.02 (1H, s, H-8) and 8.57 (1H, s, H-4); ^{13}C NMR (100 MHz, MeOD-d_4 and $CDCl_3$): δ_C 108.0 (C-3), 114.8 (CN), 123.6 (C-10), 127.9 (C-8), 129.3 (C-5), 130.0 (C-6), 140.4 (C-7), 144.7 (C-4), 148.4 (C -9) and 149.6 (C-2).

*2.2.6. Synthesis of 2,7-Dichloroquinoline-3-carboxamide (**6**).* A 100 mL round-bottom flask was charged with 2,7-dichloroquinoline-3-carbonitrile (0.19 g, 0.85 mmol), acetic acid (2 mL), and sulfuric acid (1 mL). The mixture was refluxed using a water condenser with stirring for 3 hrs, and the progress of the reaction was monitored with TLC. After completion of the reaction, the mixture was cooled and poured into a beaker containing 100 mL of ice water. The dark crystal was collected by suction filtration and mp 206–208°C; yield 0.15 g (73%); TLC : R_f = 0.77 (CH_2Cl_2 : MeOH, 9 : 1); UV-Vis: λmax (DMSO) 261 nm; MS (EI, 70 eV) m/z 241; ^{1}H NMR (400 MHz, DMSO-d_6): δ_H 7.30 (1H, J = 12.00 Hz, d, H-6), 7.94 (1H, J = 8.00 Hz, d, H-5), 8.82 (1H, s, H-8), 8.98 (1H, s, H-4) and 12.42 (broad, NH_2 proton); ^{13}C NMR (100 MHz, DMSO-d_6): δ_C 115.0 (C-8), 117.8 (C-10), 122.9 (C-3), 123.4 (C-6), 132.0 (C-5), 137.5 (C-7), 140.8 (C-9), 144.1 (C-4), 162.3 (C-2), and 164.3 (carbonyl carbon).

*2.2.7. Synthesis of 7-Chloro-2-methoxyquinoline-3-carbaldehyde (**7**).* A 100 mL round-bottom flask was charged with 2,7-dichloroquinoline-3-caraldehyde (0.99 g, 4.4 mmol), methanol (10 mL), N,N-dimethylformamide (13 mL), and potassium carbonate (0.57 g, 8.8 mmol). The mixture was refluxed using a water condenser with stirring for 4 hrs, and the progress of the reaction was monitored by TLC. After completion of the reaction, the mixture was cooled to room temperature and poured into 60 ml crushed ice water. The yellow crystal was collected using suction filtration and mp 102–104°C; yield 74% with R_f = 0.71 (n-hexane:ethyl acetate = 5 : 1). UV-Vis λmax (MeOH) 368 nm; MS (EI, 70 eV) m/z 221.5; ^{1}H NMR (400 MHz, MeOD-d_4 and $CDCl_3$): δ_H 4.09 (3H, s, methoxy proton), 7.30 (1H, s, H-6), 7.65 (1H, s, H-5) 7.72 (1H, s, H-8), 8.44 (1H, s, H-4) and 10.32 (1H, s, aldehyde proton); ^{13}C NMR (100 MHz, MeOD-d_4 and $CDCl_3$): δ_C 53.6 (methoxy carbon), 119.6 (C-3), 122.4 (C-10), 124.7 (C-6), 125.8 (C-8), 130.5 (C-5), 137.7 (C-7), 139.5 (C-4), 149.0 (C-9), 161.5 (C-2) and 188.9 (carbonyl carbon).

*2.2.8. Synthesis of 7-Chloro-2-ethoxyquinoline-3-carbaldehyde (**8**).* A 100 mL round bottom flask was charged with 2,7-dichloroquinoline-3-carbaldehyde (0.5 g, 2.2 mmol), potassium carbonate (0.6 g, 4.3 mmol), ethanol (10 mL), and N,N-dimethylformamide (10 mL). The mixture was refluxed using a water condenser with stirring for 4 hrs, and the progress of the reaction was monitored by TLC. At the end, ethanol was removed by distillation, and the remaining cooled mixture was poured into 80 mL crushed ice water. The solid product was collected by suction filtration, and the yield was 0.35 g (67%); mp 94–96°C with R_f = 0.75 (n-hexane: ethyl acetate, 4 : 1); UV-Vis λmax (MeOH) 379 nm; MS (EI, 70 eV) m/z 235.5; ^{1}H NMR (400 MHz, $CDCl_3$): δ_H 1.50 (3H, t, J = 6.00 Hz, methyl), 4.61 (2H, q, J = 8.00 Hz, methylene), 7.33 (1H, d, J = 12.00 Hz, H-6), 7.71 (1H, d, J = 8.00 Hz, H-5), 7.80 (1H, s, H-8), 8.48 (1H, s, H-4) and 10.44 (1H, s, aldehyde proton); ^{13}C NMR (100 MHz, $CDCl_3$): δ_C 14.4 (CH_3), 62.7 (OCH_2), 119.9 (C-3), 122.6 (C-10), 125.9 (C-6), 126.5 (C-8), 130.7 (C-5), 138.6 (C-7), 139.1 (C-4), 149.4 (C-9), 161.6 (C-2) and 189.0 (carbonyl carbon).

*2.2.9. Synthesis of 2-Chloroquinoline-3-carbonitrile (**12**).* In a test tube, 2-chloroquinoline-3-carbaldehyde (1 g, 5.2 mmol), sodium azide (0.68 g, 10.5 mmol), and phosphorus oxychloride (4 mL, 42.7 mmol) of ratio 1 : 1: 5 were added and stirred for 30 minutes in a hood. The mixture was heated in a water bath for 6 hrs, and the reaction progress was monitored by TLC. After completion of the reaction, the mixture was cooled to room temperature and poured into a

beaker containing 60 mL of crushed ice water. The yellow crystal was collected by suction filtration, mp 132–134°C; yield 89% with $R_f = 0.66$ (n-hexane: ethyl acetate = 5 : 1). The product was purified over silica gel column chromatography n-hexane: ethyl acetate (3 : 1) as eluent. UV-Vis λmax (MeOH) 357 nm; MS (EI, 70 eV) m/z 188.5; ^{1}H NMR (400 MHz, $CDCl_3$): δ_H 7.32 (1H, s, H-4), 7.75 (1H, t, $J = 6$ Hz, H-6), 7.96 (1H, t, $J = 8.00$ Hz, H-7), 8.10 (1H, d, $J = 8.00$ Hz, H-5) and 8.60 (1H, d, H-8); ^{13}C NMR (100 MHz, $CDCl_3$): δ_C 107.9 (C-3), 115.1 (C triple bond N), 125.1 (C-10), 128.1 (C-8), 128.8 (C-5), 128.9 (C-6),133.7 (C-7), 144.9 (C-4), 148.2 (C-9) and 148.2.

2.3. Antibacterial Activity. The *in vitro* antibacterial activity of the compounds synthesized was determined by the disc diffusion method against four strains of bacterial species: two Gram-positive (*S. aureus* (ATCC25923), *S. pyogenes* (ATCC19615)) and two Gram-negative (*E. coli* (ATCC25922), *P. aeruginosa* (ATCC27853)). The medium was prepared by dissolving Mueller Hinton Agar (MHA) in distilled water and then autoclaved at 121°C for 15 min. It was poured into sterile plates (20–25 mL/plate), and the plates were allowed to solidify under a sterile condition at room temperature.

The synthesized compounds at the concentrations of 100 and 200 μg/mL were prepared by dissolving the samples in dimethyl sulphoxide (DMSO). The sterile discs (6 mm) were infused with the synthesized compounds, positioned on the surface of the medium with sterile forceps, and gently pressed down to ensure contact with the MHA [21]. After incubation for 24 hrs at 37°C, the inhibition zone produced by the synthesized compounds was evaluated by measuring the diameter (mm) of the clear zone around the disc against the test organisms using a ruler. Amoxicillin was used as a standard antibiotic, and DMSO was used as a control.

2.4. Radical Scavenging Activity. The diphenyl picryl hydride (DPPH) radical scavenging activity of the synthesized compounds was assessed following the previously reported procedure [22]. In short, 0.04 mg/mL (0.004% (w/v)) solution of DPPH in methanol was prepared and used as control solution. The synthesized compounds were serially diluted in DPPH solution to furnish four different concentrations (1.25, 2.50, 5.00, and 10.00 μg/mL). This was repeated for ascorbic acid, used as standard. After a 30 min incubation period at room temperature, the absorbance was measured against blank at λ_{max} 517 nm [23]. The activity was expressed as % inhibition and IC_{50}, the concentration of the sample that can scavenge 50% of DPPH free radical. The percent DPPH inhibition (%I) of the compounds synthesized and ascorbic acid was calculated by the following formula:

$$\%\, I = \frac{(\text{A control} - \text{A sample})}{\text{A control}} \times 100, \quad (1)$$

where A control is the absorbance of the control reaction and A sample is the absorbance of the test compound.

2.5. In Silico Molecular Docking Analysis. AutoDock Vina with the standard protocol was used to dock the proteins (PDB ID : 6F86; PDB ID : 4FM9, and PDB ID : 1HD2) and synthesized compounds incorporated into the active site of proteins. The chemical structures of compounds were drawn using the ChemOffice tool (ChemDraw 16.0) assigned with proper 2D orientation, and the energy of each molecule was minimized using ChemBio3D. The energy-minimized ligand molecules were then used as input for AutoDock Vina to carry out the docking simulation. The crystal structures of receptor molecule *E. coli* gyrase B (PDB ID : 6F86) and human topoisomerase IIβ (4fm9) were downloaded from the protein data bank. The protein preparation was done using the reported standard protocol by removing the cocrystallized ligand, selected water molecules, and cofactors; the target protein file was prepared by leaving the associated residue with protein using Auto preparation of target protein file AutoDock 4.2 (MGLTools 1.5.6). The graphical user interface program was used to set the grid box for docking simulations. The graphical user interface program was used to set the grid box for docking simulations. The grid box was constructed using 40, 40, and 40, pointing in *x*, *y*, and *z* directions, respectively, with a grid point spacing of 0.375 Å. The center grid box was (13.52 Å, 15.68 Å, and 19.12 Å), (16.40 Å, 39.73 Å, and 23.10 Å), and (18.04 Å, 20.67 Å, and 17.69 Å), for 6f86, 4fm9, and 1hd2, respectively. The docking algorithm provided with AutoDock Vina was used to search for the best-docked conformation between ligand and protein. During the docking process, a maximum of nine conformers were considered for each ligand. The conformations with the most favorable (least) free binding energy were selected for analyzing the interactions between the target receptor and ligands by Discovery Studio Visualizer and PyMOL. The ligands are represented in different colors. H-bonds and the interacting residues are represented in ball and stick model representation [24].

2.5.1. In Silico Drug-Likeness and Toxicity Predictions. Drug-likeness properties of the compounds synthesized were predicted based on an already established concept by Lipinski's rule [25]. The structures of the synthesized compounds were converted to their canonical simplified molecular-input line-entry system (SMILE). These compounds were submitted to the SwissADME and PreADMET tool to estimate *in silico* pharmacokinetics, such as the number of hydrogen donors, hydrogen acceptors, rotatable bonds, and total polar surface area of a compound. The organ toxicities and toxicological endpoints of the synthesized compounds were predicted using PreADMET and OSIRIS Property. The analyses of the compounds were compared with that of the clinical drug (vosaroxin/ciprofloxacin), and only compounds without violation of any screening were used for the molecular docking analysis.

3. Results and Discussion

3.1. Synthesis. A series of quinoline derivatives were prepared in multistep reactions using different reaction conditions to generate novel quinoline derivatives with

antimicrobial and antioxidant properties. In this regard, treatment of 3-chloroaniline with acetic anhydride in acetic acid furnished 3-chloroacetanilide. The product was transformed to 2,7-dichloroquinoline-3-carbaldehyde (**4**) using $POCl_3$ in DMF employing a Vilsmeier reaction. Substitution of chlorine in position 2 of quinoline (**4**) with methoxy and ethoxy was accomplished by refluxing 2,7-dichloroquinoline-3-carbaldehyde (**4**) in DMF with methanol and ethanol as nucleophile and potassium carbonate as a base to afford 2-chloro-2-methoxyquinoline-3-carbaldehyde (**7**) and 7-chloro-2-ethoxyquinoline-3-carbaldehyde (**8**), respectively. On the contrary, 2-chloroquinoline-3-carbaldehyde (**11**) was prepared from acetanilide and converted to 2-chloroquinoline-3-carbonitrile (**12**) in 89% yield using sodium azide and phosphorous oxychloride. The yield was superior compared with the same compound synthesized by Mekheimer et al., 2019 [26]. On the contrary, treatment of 2,7-dichloroquinoline-3-carbaldehyde (**4**) with sodium azide in phosphorus oxychloride to afforded 2,7-dichloroquinoline-3-carbonitrile (**5**) in 64% yield. Compound **5** was further transformed into 2,7-dichloroquinoline-3-carboxamide (**6**) by refluxing acetic acid and sulfuric acid. The overall sequence of reactions used in the synthesis of various targeted quinoline derivatives is illustrated in Schemes 1 and 2.

3.2. Antibacterial Activity. Quinolines are pharmacologically active compounds used to treat various life-threatening diseases [19]. In an attempt to find bioactive quinoline analogs, a series of quinoline derivatives were synthesized and tested for their antibacterial activity against some Gram-positive and Gram-negative bacterial pathogens by measuring the inhibitory effect of such compounds. The results are described in Table 1 and Figure 1.

All synthesized compounds displayed weak-to-moderate activities against all tested bacterial strains when compared with amoxicillin, a standard drug used in the present study. The mean inhibition zone exhibited by the synthesized compounds ranged from 7.00 ± 0.04 to 12.00 ± 0.00 mm. Compounds **6** and **8** showed good activities against *E. coli* with mean inhibition zones of 11.00 ± 0.04 and 12.00 ± 0.00 mm, respectively, while compound **5** exhibited good activity against *S. aureus* and *P. aeruginosa* with 11.00 ± 0.03 mm at 200 μg/mL. The activity shown by compound **8** is superior to the other compounds synthesized in the present study but modest compared with standard amoxicillin. On the contrary, compound **7** showed better activity against *S. pyogenes* with mean inhibition of 11.00 ± 0.02 mm compared with the other synthesized compounds at 200 μg/mL. Compound **7** also displayed a medium inhibition zone against all strains of bacteria used in this study except for *S. pyogenes*. Compounds **5** and **8** showed medium activities against other tested strains of bacteria, while compound **12** showed a medium mean inhibition zone against three other tested bacterial strains such as *S. aureus, P. aeruginosa*, and *S. pyogenes*. The activity displayed by compound **12** against *P. aeruginosa* in this work contradicted with previous work reported as inactive by Kamal et al. [27]. The synthesized compounds have stronger activities when compared with related compounds reported in [19], which differ in substituents and functional groups. The better activity shown by these compounds might be due to chlorine at 7-position and the amide and nitrile functional groups.

3.3. Radical Scavenging Activity. Antioxidants are substances that prevent and stabilize the damage caused by free radicals via supplying their own electrons to these damaged cells. Antioxidants also turn free radicals into waste by-products, which are eliminated from the body [28]. DPPH assay is a quick method to evaluate the radical scavenging activity of the samples. Compounds exhibiting antioxidant activity reduced the absorbance at 517 nm, which is due to DPPH radical. Furthermore, antioxidants turn the purple color due to DPPH radical to yellow or colorless. In this work, the radical scavenging activity of the compounds synthesized was evaluated using DPPH, and the findings are depicted in Table 2 and Figure 2. Moreover, the IC_{50} values of the synthesized compounds were calculated using Microsoft Excel, and the results are summarized in Figure 3.

The DPPH radical scavenging activity of the synthesized compounds was compared with ascorbic acid, which was used as standard, and the result is graphically presented in Figure 2.

Generally, the antioxidant activities of the synthesized compounds in this work were medium to high relative to ascorbic acid at the same concentration. The radical scavenging activity of compound **6** was found to be 68.82%. The result was better than the activity displayed by the other synthesized compounds. Moreover, the percentage free radical inhibition of compound **6** at 2.50 and 1.25 μg/mL was much significant compared with the results shown by ascorbic acid. This was supported by the low IC_{50} of compound **6** (0.31 μg/mL) compared with ascorbic acid (2.41 μg/mL). The percentage inhibition of compound **8** at 10.00 μg/mL, 5.00 μg/mL, and 2.50 μg/mL is medium when compared with that of ascorbic acid and high in 1.25 μg/mL concentration. The IC_{50} value shown by compound **5** was 2.17 μg/mL. This is superior relative to ascorbic acid used as the positive control. This might be because of the presence of free electrons in the amide functional group in compound **5**. The percentage inhibition of compound **7** is almost low in all concentrations relative to ascorbic acid. Compound **12** does not have percentage inhibition at all tested concentrations. 1,1-Diphenyl-2-picrylhydrazyl (DPPH) is a stable free radical accepting hydrogen from a corresponding donor, which causes it to lose the characteristic deep purple (λ_{max} 517 nm) color. Compound **6** contains an ethoxy group at 2-position, which is responsible for accepting free radicals from DPPH. The synthesized compounds have stronger activities when compared with related compounds reported in the literature, which differ in substituents and functional groups. These were due to the presence of proton and other groups, which were accepting radicals from DPPH.

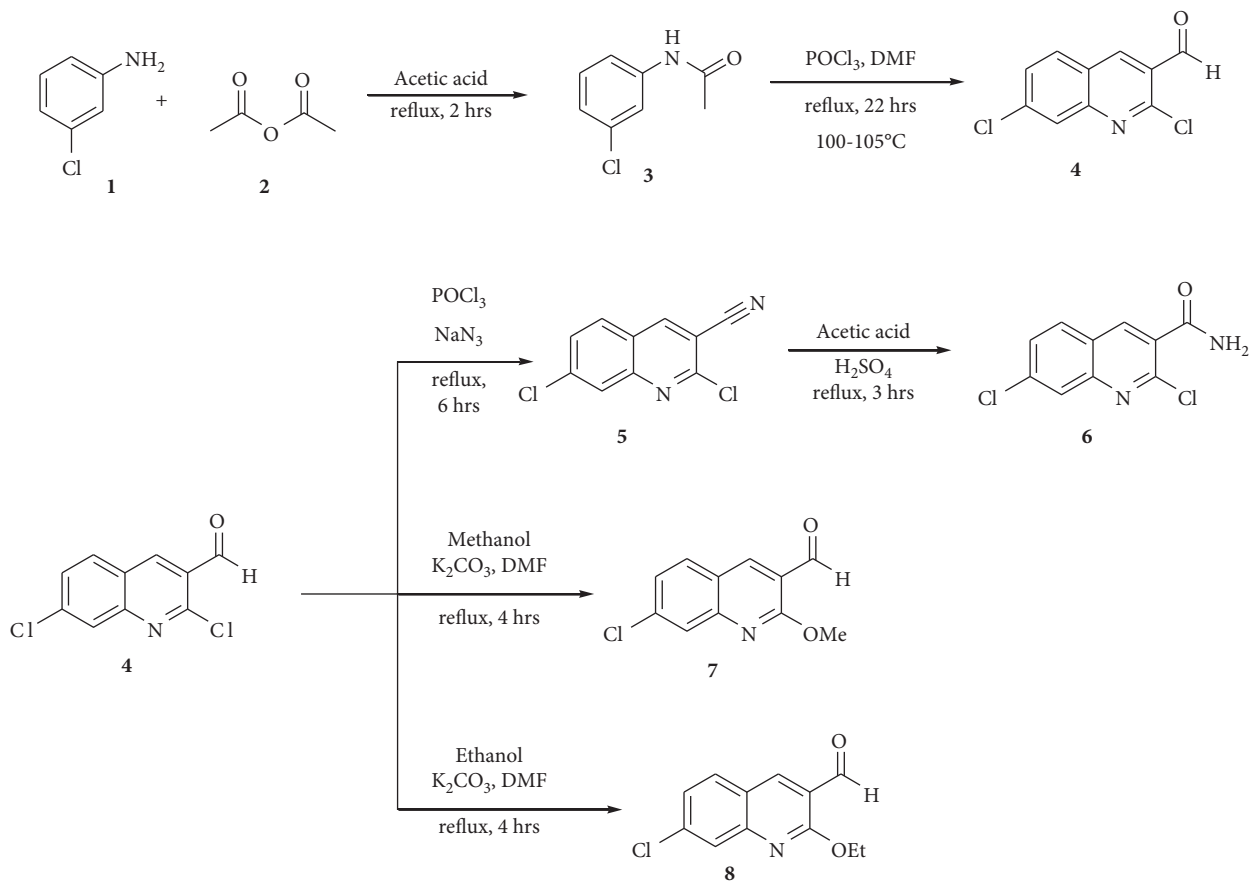

Scheme 1: Synthesis of 7-chloroquinoline-3-carbaldehyde and its derivatives.

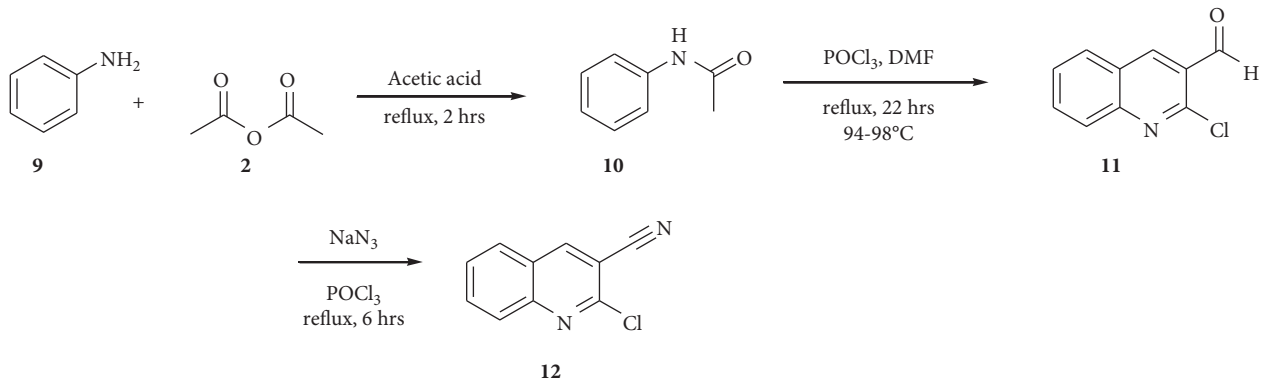

Scheme 2: Synthesis of 2-chloroquinoline-3-carbonitrile (**12**).

3.4. In Silico Molecular Docking Analysis against E. coli DNA Gyrase B. The DNA gyrase, an enzyme belonging to a member of bacterial topoisomerase, controls the topology of DNA during transcription, replication, and recombination by introducing transient breaks to both DNA strands. In this regard, bacterial DNA gyrase is essential for bacterial survival and, therefore, necessary to be exploited as an antibacterial drug target [29]. Thus, in this study, the molecular docking analysis of the synthesized compounds was conducted to investigate their binding pattern with DNA gyrase and compared them with ciprofloxacin used as a standard drug. The synthesized compounds (**5**–**8** and **12**) were found to have minimum binding energy ranging from −6.1 to −6.6 kcal/mol (Table 3), with is better achieved using compound **8** (−6.6 kcal/mol). The binding affinity, H-bond, and residual interaction of five compounds and ciprofloxacin are summarized in Table 3.

Compared to ciprofloxacin, the synthesized compounds (**5**, **6**, and **12**) showed similar residual interactions (Van der Waals interaction) with amino acid residues Ala-47 and hydrophobic interaction with amino acid residues Ile-78, and

Table 1: The inhibition zone of synthetic compounds in mm (mean ± SD).

Compounds	Concentrations in μg/mL	Bacteria strains and zone of inhibition in mm			
		E. coli	*S. aureus*	*P. aeruginosa*	*S. pyogenes*
5	100	7.00 ± 0.04	9.00 ± 0.03	9.00 ± 0.04	8.00 ± 0.01
	200	9.00 ± 0.01	11.00 ± 0.03	11.00 ± 0.03	10.00 ± 0.04
6	100	9.00 ± 0.00	8.00 ± 0.01	7.00 ± 0.04	7.00 ± 0.01
	200	11.00 ± 0.04	9.00 ± 0.00	8.00 ± 0.01	8.00 ± 0.03
7	100	8.00 ± 0.00	8.00 ± 0.00	8.00 ± 0.03	10.00 ± 0.04
	200	10.00 ± 0.01	9.00 ± 0.01	9.00 ± 0.04	11.00 ± 0.02
8	100	10.00 ± 0.00	8.00 ± 0.01	9.00 ± 0.04	7.00 ± 0.03
	200	12.00 ± 0.00	9.00 ± 0.04	10.00 ± 0.00	10.00 ± 0.03
12	100	8.00 ± 0.02	7.00 ± 0.01	8.00 ± 0.00	8.00 ± 0.02
	200	9.00 ± 0.04	10.00 ± 0.01	8.00 ± 0.00	9.00 ± 0.02
Amoxicillin	100	16.00 ± 0.00	15.00 ± 0.01	16.00 ± 0.04	16.00 ± 0.03
	200	18.00 ± 0.01	17.00 ± 0.01	18.00 ± 0.00	18.00 ± 0.03

Results are mean ± SD of duplicate experiments. Amoxicillin was used as a positive control.

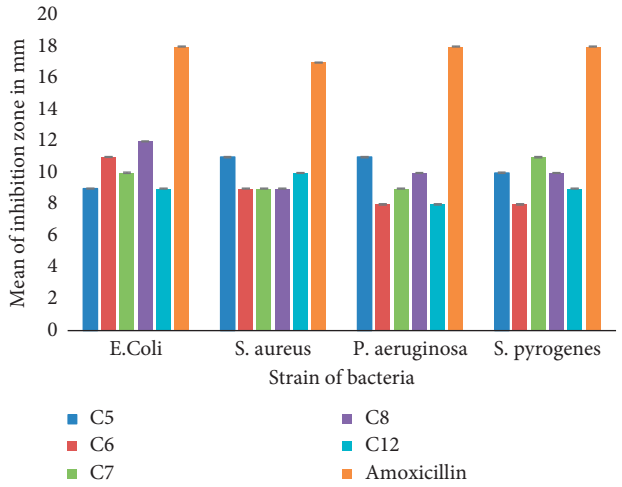

Figure 1: The inhibition zone of the synthetic compounds in mm (mean ± SD) at 200 μg/mL. Results are mean ± SD of duplicate experiments. Amoxicillin was used as positive control; C compounds.

Table 2: Percentage inhibition and IC_{50} of synthesized compounds and ascorbic acid.

Conc.	% radical inhibition of compounds 5–8					
μg/mL	4	5	6	7	8	Ascorbic acid
10.00	16.92	50.77	68.82	13.08	55.00	91.15
5.00	14.62	10.77	67.70	9.62	21.54	73.08
2.50	14.00	5.38	65.45	5.77	15.00	35.00
1.25	11.92	4.23	65.17	4.62	13.85	11.15
IC_{50} (mol/L)	74.72	2.17	0.31	16.78	4.32	2.41

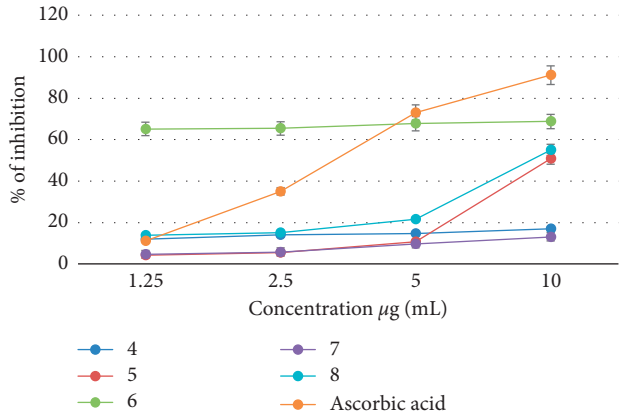

Figure 2: The percentage inhibition of free radical DPPH by the synthesized compounds.

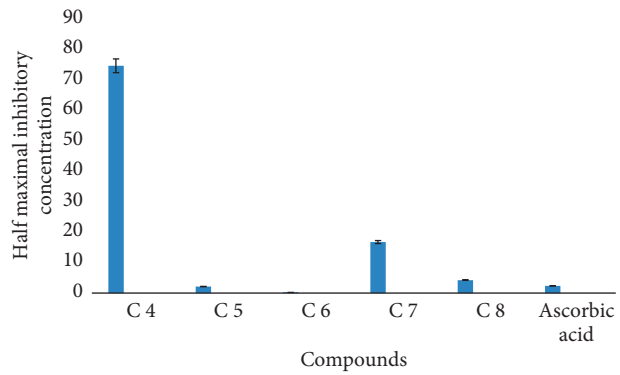

Figure 3: The IC50 values of the synthesized compounds.

compounds **5** and **6**, and **7** and **8** showed similar hydrophobic interactions with amino acid residues Glu-50 and Asn-46, respectively. Compounds **6**, **7**, and **8** showed additional hydrogen-bonding interactions with amino acid residues Asp-73, and compounds **7** (Arg-76) and **8** (Thr-165) showed additional hydrogen-bonding interactions with amino acid residues. The findings of the *in silico* molecular docking analysis match with the *in vitro* antibacterial activity of the synthesized compounds. Among the compounds synthesized, compounds **6** (−6.4 kcal/mol) and **8** (−6.6 kcal/mol) had better activity compared with the others. The synthesized compounds have minimum binding energy when compared with related compounds reported in [19], which differ in substituents and functional groups. These were due to chlorine substituted at 7-position and the amide and nitrile functional groups. The 3-dimensional binding interaction of compounds **6, 8** and that of ciprofloxacin against *E. coli* gyrase B complex are illustrated in Figures 4–6.

Table 3: Molecular docking value of synthetic compounds against *E. coli* DNA gyrase B.

Compounds	Affinity (kcal/mol)	H-bond	Residual amino acid interactions	
			Hydrophobic/Pi-cation/Pi-anion/Pi-alkyl interactions	Van der Waals interactions
5	−6.1	Gly-77	Asp-73, Glu-50, Ile-78, Ile-94	Ala-47, Arg-76, Gly-75, Pro-79, Asn-46, Thr-165
6	−6.4	Asp-73, Asn-46, Gly-77	Glu-50, Pro-79, Ile-78, Arg-76	Ala-47, Gly-75, Thr-165
7	−6.3	Asp-73, Arg-76, Gly-77	Ala-47, Ile-78, Asn-46, Ile-94	Glu-50, Gly-75
8	−6.6	Asp-73, Gly-77, Thr-165	Ala-47, Ile-78, Asn-46, Ile-94	Glu-50, Val-43, Pro-79
12	−6.2	Gly-77	Asp-73, Ile-78, Ile-94	Ala-47, Glu-50, Asn-46, Gly-75, Pro-79
Ciprofloxacin	−7.2	Asp-73, Arg-76, Thr-165	Glu-50, Gly-77, Ile-78, Asn-46	Ala-47

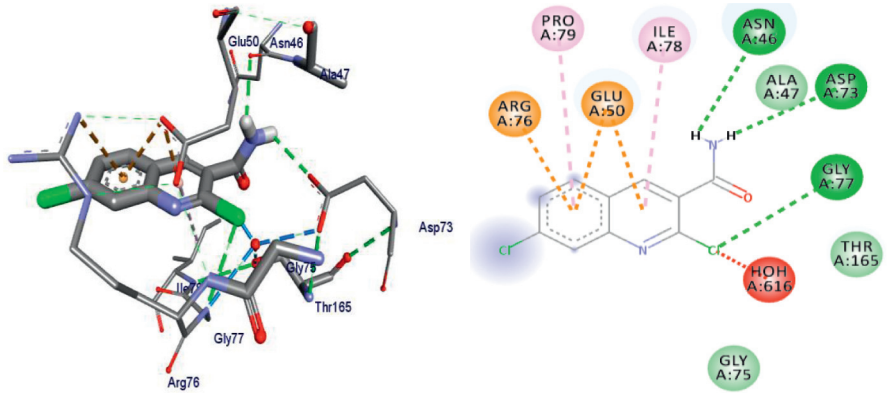

Figure 4: The binding interactions of compound 6 against *E. coli* DNA gyrase B (PDB ID : 6F86).

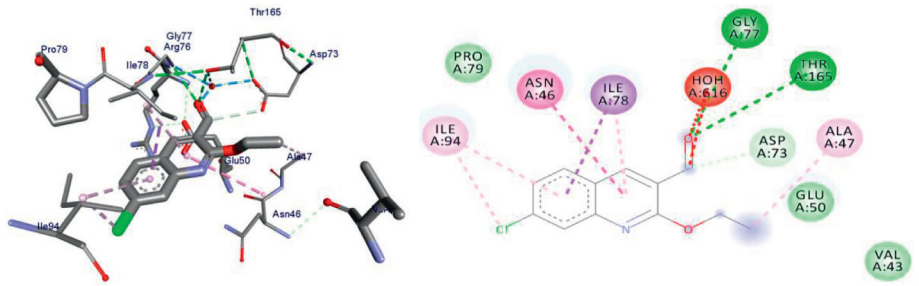

Figure 5: The binding interactions of compound 8 against *E. coli* DNA gyrase B (PDB ID : 6F86).

3.5. In Silico Molecular Docking Analysis against Human Topoisomerase IIβ. Topoisomerase II is an enzyme belonging to a human topoisomerase that cuts both strands of the DNA helix simultaneously to manage DNA tangles and supercoils [30]. Human DNA topoisomerase II is an important target in anticancer therapy. The human topoisomerase II is crucial to control the topology of DNA during replication, transcription, and recombination by introducing temporary breaks to both DNA strands. Therefore, in this study, the molecular docking analysis of the synthesized compounds was conducted to investigate their binding pattern with DNA topoisomerase IIβ and compare them with a standard drug (vosaroxin), which is an anticancer drug.

The synthesized compounds were found to have minimum binding energy ranging from −6.9 to −7.3 kcal/mol (Table 4), best results achieved with compound **8** (−7.3 kcal/mol), **5** (−7.1 kcal/mol), and **6** (−7.1 kcal/mol). The binding affinity, H-bond, and residual interaction of five compounds and vosaroxin were summarized in Table 4.

Compared to vosaroxin, the synthesized compounds (**5**, **6**, **7**, and **12**) showed similar residual interactions (Van der Waals interaction) with amino acid residues Tyr-684, compound **12** with Gln-542. Compounds **5**–**8** showed similar residual interactions (hydrophobic interactions) with amino acid residues Leu-705 and Pro-593, and compound **12** showed similar hydrophobic interactions with amino acid

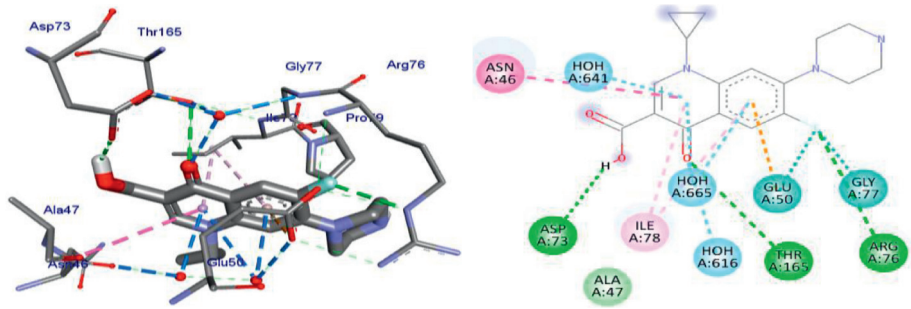

Figure 6: The binding interactions of ciprofloxacin against *E. coli* DNA gyrase B (PDB ID : 6F86).

Table 4: Molecular docking value of synthesized compounds against Human Topoisomerase IIβ (PDB ID: 4fm9).

Compounds	Affinity (kcal/mol)	Residual amino acid interactions		
		H-bond	Hydrophobic/Pi-cation/ Pi-anion/Pi-alkyl interactions	Van der Waals interactions
5	−7.1	--	Pro-593, Leu-705, Gln-542	Asp-541, Glu-702, Lys-550, Ser-547, Asp-543, Gln-544, Asp-683, Tyr-684
6	−7.1	Leu-685, Gln-542	Leu-705, Pro-593, Lys-701, Tyr-686	Asp-683, Tyr-684, Glu-702, Ser-547, Tyr-590
7	−6.9	Ser-547, Leu-685, Gln-542	Pro-593, Leu-705, Lys-701	Asp-683, Tyr-684, Leu-592, Ser-591, Tyr-590, Ile-577
8	−7.3	Ser-591, Leu-685, Glu-702, Tyr-590, Leu-592, Gln-542	Pro-593, Leu-705, Lys-701	Asp-683, Asp-543, Ile-577
12	−7.0	Leu-685	Ile-577, Tyr-686, Leu-705	Ser-547, Lys-550, Gln-542, Tyr-590, Ser-591, Tyr-684, Lys-701, Glu-702
Vosaroxin	−7.2	Ser-591, Leu-685, Leu-592	Leu-705, Ile-577, Pro-593	Glu-682, Tyr-684, Arg-672, Gln-542

residues Leu-705 and Ile-577. Compound **8** showed additional hydrogen-bonding interactions with amino acid residues Ser-591 and Leu-685, and compounds **6**, **7**, and **12** also showed additional hydrogen-bonding interactions with amino acid residues Leu-685. Compounds **5** and **6**'s docking results partially matched the vosaroxin interactions with amino acid residues. The docking result of compound **8** was found to be stronger than that vosaroxin. Therefore, compounds **5, 6**, and **8** might have the best anticancer agents among the synthesized compounds in this study. The 3-dimensional binding interaction of compounds **5, 6, 8**, and vosaroxin against human topoisomerase IIβ is illustrated in Figures 7–10.

A drug-likeness prediction model introduced by Hu et al. involved molecular descriptors related to numbers of different atom types and decision trees for discriminating between potential drugs and nondrugs [31]. ADME describes the disposition and fate of pharmaceutical compounds within an organism, especially in the human body [32]. The primary cause of failure during the drug development phase is poor pharmacokinetics (PK) and toxicity rather than poor efficacy of the candidate compound. The prediction of compound toxicities is an important part of the drug design development process. ProTox-II incorporates molecular similarity, fragment propensities, most frequent features, and machine learning, based a total of 33 models for the prediction of various toxicity endpoints such as acute toxicity, hepatotoxicity, cytotoxicity, carcinogenicity, mutagenicity, immunotoxicity, adverse outcomes pathways, and toxicity targets [33].

The SwissADME predicted results showed that the synthesized compounds **5**–**8** and **12** satisfy Lipinski's rule of five with zero violations for their drug-like molecular nature (Table 5). According to Lipinski's rule of five, the molecular weight of the molecules should be less than 500, number of hydrogen bond acceptors less than ten, number of hydrogen bond donors less than five, and the lipophilicity (cLogP) values less than five [25]. The SwissADME predicted LogP values ranged from 1.85 to 2.37, assuring optimal lipophilicity of the synthesized compounds. The predicted TPSA value in (Å^2) for synthesized compounds ranged from 36.68 to 55.98, inferring very good absorption. It has been suggested that molecules with a TPSA of 140 Å^2 and above would be poorly absorbed (<10 percent fractional absorption), while compounds with a TPSA less than 60 Å^2 would be well absorbed (>90 percent) [34].

Pharmacokinetically, all synthesized compounds have high GI absorption, blood–brain barrier (BBB) permeability, and medium skin permeation value, and none of the synthesized compounds were predicted as P-glycoprotein substrate (Table 6). Under normal physiological conditions, the substance entering the brain requires being lipid-soluble, less than 400 daltons, and not substrate of active efflux transporters (AET). In this study, all synthesized compounds can pass through blood–brain barrier. Besides, the interaction of therapeutic molecules with cytochromes P450 (CYP) isoforms as a substrate of these enzymes was proposed to screen a therapeutically active molecule. It is reported that the inhibition of CYP isoenzymes is certainly one

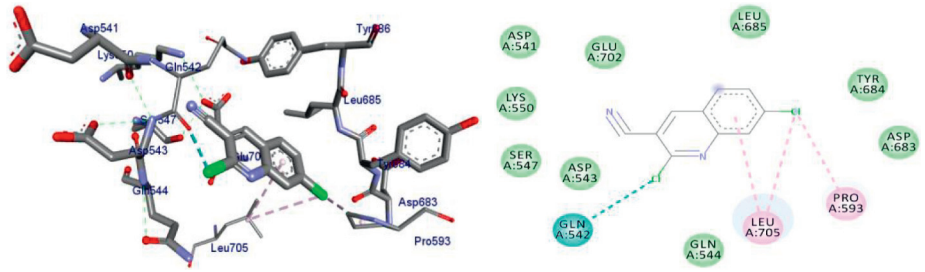

Figure 7: The binding interactions of compound 5 against human topoisomerase IIα (PDB ID: 4fm9).

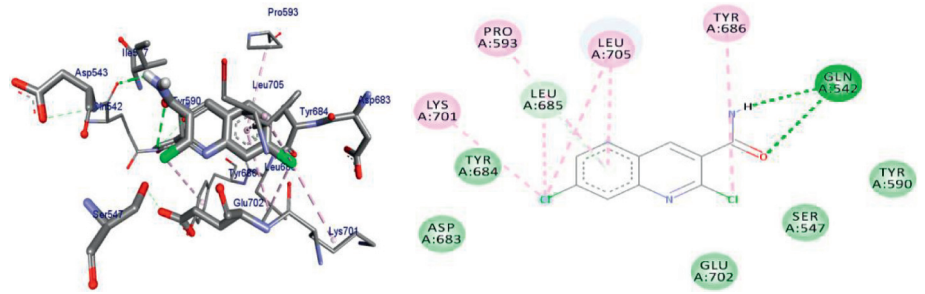

Figure 8: The binding interactions of compound 6 against human topoisomerase IIα (PDB ID: 4fm9).

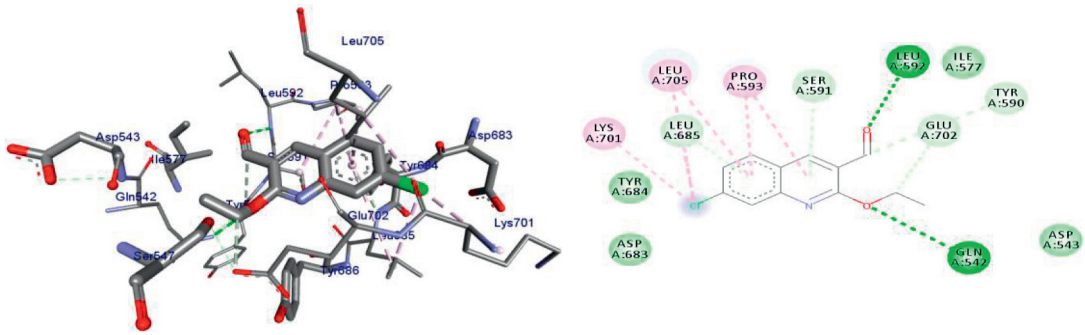

Figure 9: The binding interactions of compound 8 against human topoisomerase IIα (PDB ID: 4fm9).

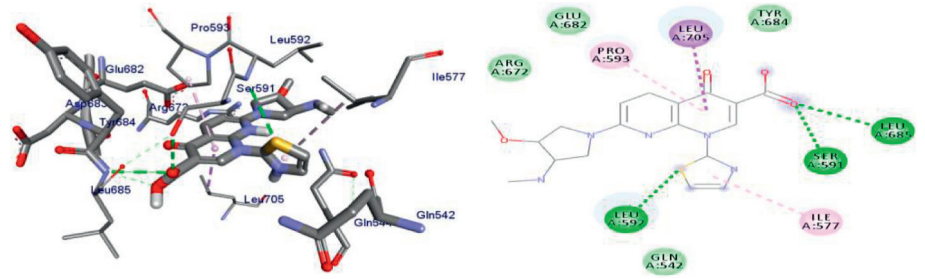

Figure 10: The binding interactions of vosaroxin against human topoisomerase IIα (PDB ID: 4fm9).

major cause of pharmacokinetics-related drug-drug interactions thereby leading to toxic or adverse effects due to the lower clearance and accumulation of the drug or its metabolites [35]. The synthesized compounds were none inhibitors of three enzymes, namely, CYP2C9, CYP2D6, and CYP3A4, and inhibitors of CYP1A2 and CYP2C19 except for compound **12** not inhibiting CYP2C19. All synthesized compounds were similar to vosaroxin in all enzymes, except for CYP2C19, which was not inhibited by compounds **5**–**8**.

The organ toxicity (hepatotoxicity) and toxicological endpoints (carcinogenicity, immunotoxicity, mutagenicity, and cytotoxicity) of the synthesized compounds were predicted with the results presented in Table 7. The ProTox II predicted organ toxicity results revealed that all the synthesized compounds were inactive in hepatotoxicity, immunotoxicity, mutagenicity, and cytotoxicity. Compounds **5**, **6**, and **12** were also inactive in carcinogenicity, and compounds **7** and **8** have carcinogenic properties.

Table 5: Drug-likeness predictions of compounds **5**–**8** and **12** computed by SwissADME.

Compounds	Formula	Mol. Wt. (g/mol)	NRB	NHA	NHD	TPSA ($A^{°2}$)	LogP (cLogP)	Lipinski's rule of five violation
5	$C_{10}H_4Cl_2N_2$	223.06	0	2	0	36.68	2.13	0
6	$C_{10}H_6C_{l2}N_2O$	241.07	1	2	1	55.98	1.85	0
7	$C_{11}H_8ClNO_2$	221.64	2	3	0	39.19	2.36	0
8	$C_{12}H_{10}ClNO_2$	235.67	3	3	0	39.19	2.37	0
12	$C_{10}H_5ClN_2$	188.61	0	2	0	36.68	1.91	0
Vosaroxin	$C_{18}H_{19}N_5O_4S$	401.45	5	9	2	136.13	0.963	0

NHD: number of hydrogen donors; NHA: number of hydrogen acceptors; NRB: number of rotatable bonds; and TPSA: total polar surface area.

Table 6: ADME predictions of compounds **5**–**8** and **12** computed by SwissADME and PreADMET.

Compounds	Chemical formula	Skin permeation value (log Kp) cm/s	GI absorption	BBB permeability	Inhibitor interaction (SwissADME/PreADMET)					
					P-gp substrate	CYP1A2 inhibitor	CYP2C19 inhibitor	CYP2C9 inhibitor	CYP2D6 inhibitor	CYP3A4 inhibitor
5	$C_{10}H_4Cl_2N_2$	−5.18	High	Yes	No	Yes	Yes	No	No	No
6	$C_{10}H_6C_{l2}N_2O$	−5.88	High	Yes	No	Yes	Yes	No	No	No
7	$C_{11}H_8ClNO_2$	−5.82	High	Yes	No	Yes	Yes	No	No	No
8	$C_{12}H_{10}ClNO_2$	−5.64	High	Yes	No	Yes	Yes	No	No	No
12	$C_{10}H_5ClN_2$	−5.41	High	Yes	No	Yes	No	No	No	No
Vosaroxin	$C_{18}H_{19}N_5O_4S$	−8.98	High	No	Yes	Yes	No	No	No	No

GI: gastrointestinal; BBB: blood–brain Barrier; P-gp: P-glycoprotein; CYP: cytochrome-P.

Table 7: Toxicity prediction of compounds **5**–**8** and **12** computed by ProTox II and OSIRIS Property Explorer.

Samples	Formula	LD_{50} (mg/kg)	Toxicity class	Organ toxicity				
				Hepatotoxicity	Carcinogenicity	Immunotoxicity	Mutagenicity	Cytotoxicity
5	$C_{10}H_4Cl_2N_2$	5000	5	Inactive	Inactive	Inactive	Inactive	Inactive
6	$C_{10}H_6C_{l2}N_2O$	705	4	Inactive	Inactive	Inactive	Inactive	Inactive
7	$C_{11}H_8ClNO_2$	2190	5	Inactive	Active	Inactive	Inactive	Inactive
8	$C_{12}H_{10}ClNO_2$	2190	5	Inactive	Active	Inactive	Inactive	Inactive
12	$C_{10}H_5ClN_2$	1100	4	Inactive	Inactive	Inactive	Inactive	Inactive
Vosaroxin	$C_{18}H_{19}N_5O_4S$	500	4	Active	Inactive	Inactive	Inactive	Inactive

Almost all synthesized compounds are similar to vosaroxin in immunotoxicity, mutagenicity, cytotoxicity, and carcinogenicity properties, but none hepatotoxicity, whereas vosaroxin was hepatotoxic. LD_{50} is the amount of substance given all at once, which causes the death of 50% (one-half) of a group of tested animals. It is one way to measure the acute toxicity of materials. The order of toxicity of synthesized compounds toward human body **6** ($LD_{50} = 705$) > **12** ($LD_{50} = 1100$) > **7** and **8** ($LD_{50} = 2190$) > **5** ($LD_{50} = 5000$). The "Lethal Dose" of compound **5** was higher than other synthesized compounds, whereas compound **6** was the least. In this study, the "Lethal Dose" of compound **6** was closer to control (vosaroxin) than other synthesized compounds.

4. Conclusion

In conclusion, five novel chloroquinoline derivatives were synthesized and characterized. The antibacterial activities of the compounds synthesized were assessed against two Gram-negative and two Gram-positive bacteria, and most of them were found to have weak-to-moderate activities against the bacterial strains used for the screening. The inhibition zone displayed by compounds **6** and **8** against *E. coli* was significant compared with the others. These compounds showed a better binding affinity with *E. coli* DNA gyrase in their *in silico* molecular docking analysis. This suggests compounds **6** and **8** as a candidate for further analysis as antibacterial agents. Compounds **5** and **6** displayed better antioxidant activity compared with ascorbic acid suggesting these compounds as a radical scavenger. Compound **8** showed a strong binding affinity against human topoisomerase IIβ compared with vosaroxin suggesting this compound as a lead compound for further study as an anticancer drug.

Abbreviations

ADME: Absorption, distribution, metabolism, and excretion
ATCC: American type culture collection
DNA: Deoxyribonucleic acid
DMSO: Dimethyl sulphoxide
DPPH: Diphenyl picryl hydride
E. coli: *Escherichia coli*
IC: Inhibitory concentration
%I: Percent inhibition
LD: Lethal dose
MHA: Mueller-Hinton agar

NMR: Nuclear magnetic resonance
P. aeruginosa: *Pseudomonas aeruginosa*
S. aureus: *Staphylococcus aureus*
S. pyogenes: *Streptococcus pyogenes*
TLC: Thin-layer chromatography
UV-Vis: Ultraviolet visible.

Data Availability

The data used in this study can be accessed from the corresponding author upon request. The NMR data used to support the findings of this study are incorporated as supplementary information.

Disclosure

This manuscript was extracted from the thesis of Mr. Bayan Abdi (http://etd.astu.edu.et/bitstream/handle/123456789/1770/Bayan%20Abdi%20Ahmed.pdf?isAllowed=y&sequence=1) done under the supervision of Dr. Yadessa Melaku at the Applied Chemistry Department of Adama Science and Technology University.

Conflicts of Interest

The authors declare that there are no conflicts of interest regarding the publication of this paper.

Acknowledgments

The authors are thankful to Adama Science and Technology University for funding this research with grant number ASTU/AS-R/002/2020.

Supplementary Materials

The NMR spectra (Figures 1–9) of the synthesized compounds are incorporated as supplementary information. (*Supplementary Materials*)

References

[1] M. Pigłowski, "Pathogenic and non-pathogenic microorganisms in the rapid alert system for food and feed," *International Journal of Environmental Research and Public Health*, vol. 16, p. 477, 2019.

[2] B. Mansoori, A. Mohammadi, S. Davudian, S. Shirjang, and B. Baradaran, "The different mechanisms of cancer drug resistance: a brief review," *Advanced Pharmaceutical Bulletin*, vol. 7, no. 3, pp. 339–348, 2017.

[3] N. Principi, E. Silvestri, and S. Esposito, "Advantages and limitations of bacteriophages for the treatment of bacterial infections," *Frontiers in Pharmacology*, vol. 10, pp. 1–9, 2019.

[4] R. Vivas, A. A. T. Barbosa, S. S. Dolabela, and S. Jain, "Multidrug-resistant bacteria and alternative methods to control them: an overview," *Microbial Drug Resistance*, vol. 25, no. 6, pp. 890–908, 2019.

[5] M. D. Don, "Antioxidant activity of methanol extract/fractions of *senggani leaves*," *Pharmaceutica Analytica Acta*, vol. 8, pp. 1–6, 2017.

[6] G. Pizzino, "Oxidative stress: harms and benefits for human health," *Oxidative Medicine and Cellular Longevity*, vol. 2017, Article ID 8416763, 12 pages, 2017.

[7] P. Y. Chung, "Recent advances in research of natural and synthetic bioactive quinolines," *Future Medicinal Chemistry*, vol. 7, pp. 947–967, 2015.

[8] S. B. Christensen, "Natural products that changed society," *Biomedicines*, vol. 9, p. 472, 2021.

[9] B. S. Matada, R. Pattanashettar, and N. G. Yernale, "Corrigendum to 'A comprehensive review on the biological interest of quinoline and its derivatives," *Bioorganic & Medicinal Chemistry*, vol. 32, pp. 1–11, 2021.

[10] J. J. Casal and S. E. Asís, "Austin tuberculosis: research & treatment natural and synthetic quinoline derivatives as antituberculosis agents," *Austin Tuberculosis: Research & Treatment*, vol. 2, pp. 2–4, 2017.

[11] Y. Li, J. Hu, Y. Wang, J. Zhou, L. Zhang, and Z. Liu, "DeepScaffold: A comprehensive tool for scaffold-based de Novo drug discovery using deep learning," *Journal of Chemical Information and Modeling*, vol. 60, no. 1, pp. 77–91, 2020.

[12] A. Venkanna, "Pharmacological use of a novel scaffold, anomeric N,N-diarylamino tetrahydropyran: molecular similarity search, chemocentric target profiling, and experimental evidence," *Scientific Reports*, vol. 7, pp. 1–17, 2017.

[13] K. S. Håheim, I. T. Urdal Helgeland, E. Lindbäck, and M. O. Sydnes, "Mapping the reactivity of the quinoline ring-system – synthesis of the tetracyclic ring-system of isocryptolepine and regioisomers," *Tetrahedron*, vol. 75, pp. 2949–2957, 2019.

[14] A. Tarushi, "First- and second-generation quinolone antibacterial drugs interacting with zinc(II): structure and biological perspectives," *Journal of Inorganic Biochemistry*, vol. 121, pp. 53–65, 2012.

[15] V. Yadav and P. Talwar, "Biomedicine & Pharmacotherapy Repositioning of fluoroquinolones from antibiotic to anticancer agents: an underestimated truth," *Biomedicine & Pharmacotherapy*, vol. 111, pp. 934–946, 2018.

[16] J. K. Baird, "8-Aminoquinoline therapy for latent malaria," *Clinical Microbiology Reviews*, vol. 32, pp. 1–68, 2019.

[17] S. A. Khan, A. M. Asiri, H. M. Basisi et al., "Synthesis and evaluation of Quinoline-3-carbonitrile derivatives as potential antibacterial agents," *Bioorganic Chemistry*, vol. 88, Article ID 102968, 2019.

[18] W. S. Hamama, M. E. Ibrahim, A. A. Gooda, and H. H. Zoorob, "Recent advances in the chemistry of 2- chloroquinoline-3-carbaldehyde and related analogs," *RSC Advances*, vol. 8, pp. 8484–8515, 2018.

[19] Z. Digafie, E. Rajalakshmanan, B. Zerihun, and M. Yadessa, "Synthesis and antibacterial, antioxidant, and molecular docking analysis of some novel quinoline derivatives," *Journal of Chemistry*, vol. 2020, Article ID 1324096, 16 pages, 2020.

[20] F. Bakr, Abdel-Wahab, and E. K. Rizk, "2-Chloroquinoline-3-carbaldehyde II: synthesis, reactions, and applications," *Journal of Chemistry*, vol. 2013, Article ID 851297, 13 pages, 2013.

[21] T. Peng, L. Chunhui, P. Zhong et al., "Facilely accessible quinoline derivatives as potent antibacterial agents," *Bioorganic & Medicinal Chemistry*, vol. 26, pp. 3573–3579, 2018.

[22] B. Nur, A. Azierah, M. M. Muhammad, and S. M. Khamsah, "Chemical composition and antioxidant activity of stingless bee propolis from different extraction methods," *International Journal of Engineering and Technology*, vol. 7, pp. 90–95, 2018.

[23] M. Raksha, B. Bharat, and R. Dhani, "Variation in antioxidant activity of a rattan species, *Plectocomia himalayana* griff by DPPH assay based on two different methods of methanol extraction," *Pharmacognosy and Phytochemistry*, vol. 10, no. 2, p. 175, 2018.

[24] G. Antonio, G. Laurence, S. Perrine et al., "Impact of aryloxy-linked quinazolines: a novel series of selective VEGFR-2 receptor tyrosine kinase inhibitors," *Bioorganic & Medicinal Chemistry Letters*, vol. 21, pp. 2106–2112, 2011.

[25] C. A. Lipinski, "Experimental and computational approaches to estimate solubility and permeability in drug discovery and development settings," *Advanced Drug Delivery Reviews*, vol. 23, pp. 3–25, 1997.

[26] R. Mekheimer, M. A. Al-Sheikh, H. Medrasi, and K. Sadek, "Chloroquinoline-3-carbonitriles: chemical synthesis and reactions," *Current Organic Chemistry*, vol. 23, no. 7, p. 1, 2019.

[27] Y. M. E. Kamal, F. F. Sherbiny, A. M. El-Morsi, H. E. Abu-El-khair, I. H. Eissa, and M. M. El-Sebaei, "Design, synthesis and antimicrobial evaluation of some novel quinoline derivatives," *Pharmacy & Pharmacology International Journal*, vol. 2, no. 5, pp. 165–177, 2015.

[28] M. M. Rahman, M. B. Islam, and M. Biswas, "In vitro antioxidant and free radical scavenging activity of different parts of *Tabebuia pallida* growing in Bangladesh," *BMC Research Notes*, vol. 8, p. 621, 2015.

[29] Z. Jakopin, J. Ilas, and M. Barancokova, "Discovery of substituted oxadiazoles as a novel scaffold for DNA gyrase inhibitors," *European Journal of Medicinal Chemistry*, vol. 130, pp. 171–184, 2017.

[30] V. V. Rybenkov, C. Ullsperger, A. V. Vologodskii, and N. R. Cozzarelli, "Simplification of DNA topology below equilibrium values by type II topoisomerases," *Sciences-New York*, vol. 277, pp. 690–693, 1997.

[31] Q. Hu, M. Feng, L. Lai, and J. Pei, "Prediction of drug-likeness using deep autoencoder neural networks," *Frontiers in Genetics*, vol. 9, p. 585, 2018.

[32] A. Daina1, O. Michielin, and V. Zoete, "SwissADME: a free web tool to evaluate pharmacokinetics, druglikeness and medicinal chemistry friendliness of small molecules," *Scientific Reports*, vol. 7, Article ID 42717, 2017.

[33] P. Banerjee, A. O. Eckert, A. K. Schrey, and R. Preissner, "ProTox-II: a webserver for the prediction of toxicity of chemicals," *Nucleic Acids Research*, vol. 46, pp. 257–263, 2018.

[34] D. E. Clark, "Rapid calculation of polar molecular surface area and its application to the prediction of transport phenomena. Prediction of intestinal absorption," *Journal of Pharmaceutical Sciences*, vol. 88, no. 8, pp. 807–814, 1999.

[35] P. F Hollenberg, "Characteristics and common properties of inhibitors, inducers, and activators of CYP enzymes," *Drug Metabolism Reviews*, vol. 34, no. 1-2, pp. 17–35, 2002.